Nonlinear friction-induced vibration of a slider-belt system

Zilin Li

State Key Laboratory of Structural Analysis of Industrial Equipment, Dalian University of Technology, Dalian, China

School of Engineering, University of Liverpool, Liverpool, U.K.

canydao@liverpool.ac.uk

Huajiang Ouyang[1]

State Key Laboratory of Structural Analysis of Industrial Equipment, Dalian University of Technology, Dalian, China

School of Engineering, University of Liverpool, Liverpool, U.K.

huajiang.ouyang@gmail.com

Zhenqun Guan

State Key Laboratory of Structural Analysis of Industrial Equipment, Dalian University of Technology, Dalian, China

guanzhq@dlut.edu.cn

Abstract

A mass-spring-damper slider excited into vibration in a plane by a moving rigid belt through friction is a major paradigm of friction-induced vibration. This paradigm has two aspects that can be improved: (1) the contact stiffness at the slider-belt interface is often assumed to be linear; (2) this contact is usually assumed to be maintained during vibration (even when the vibration becomes unbounded at certain conditions). In this paper, a cubic contact spring is included; loss of contact (separation) at the slider-belt interface is allowed and importantly reattachment of the slider to the belt after separation is also considered. These two features make a more realistic model of

[1]To whom all correspondence should be addressed.

friction-induced vibration and are shown to lead to very rich dynamic behaviour even though a simple Coulomb friction law is used. Both complex eigenvalue analysis of the linearised system and transient analysis of the full nonlinear system are conducted.

Eigenvalue analysis indicates that the nonlinear system can become unstable at increasing levels of the pre-load and the nonlinear stiffness, even if the corresponding linear part of the system is stable. However, they at a high enough level, become stabilising factors. Transient analysis shows that separation and reattachment could happen. Vibration can grow with the pre-load and vertical nonlinear stiffness when separation is considered, while this trend is different when separation is ignored. Finally, it is found that the vibration magnitudes of the model with separation are greater than the corresponding model without considering separation in certain conditions. Thus ignoring separation is unsafe.

Keywords: Slider-belt system, Friction-induced vibration, Self-excited, Nonlinear stiffness; Loss of contact.

1. Introduction

Generally speaking, dry friction acts as a resistance to relative motion which dissipates energy of a system; however, under certain conditions, it can cause self-excited vibration in engineering as well as in daily life [1-4], and in most of these cases is undesirable. Examples include door hinges, squeaky chalk on a blackboard, data loss of a computer hard disc drive due to flutter of the disc and a most well-known noise problem, brake squeal [5-7] that happens in the brake system of an automobile.

Various types of self-excited friction-induced vibration have been studied [1-4]. The means by which friction can excite unstable vibration are referred to as mechanisms. Several such mechanisms have been put forward and they essentially fall into the following four categories: (1) negative gradient in friction

coefficient-velocity relationship [8]; (2) sprag-slip instability, firstly proposed by Spurr [9], and also studied in [10, 11]; (3) stick-slip oscillation, which happens when the value of kinetic friction coefficient is different from the static friction [12, 13]; (4) mode-coupling instability [14-16] or mode-locking [17], which is generally acknowledged as the main mechanism for self–excited vibration in brakes. Friction was also modelled as a follower force [14, 18] or a moving load [19], or produced a friction couple [20-22]. Very recently, Elmaian et al. [7] demonstrated through numerical simulation that three typical types of brake noise (that is, creak, squeal and squeak) could be generated by one dynamics model and which type of noise actually occurred depended on the contact state ratio.

One important line of research on friction-induced vibration is establishment of the mechanisms whereby such vibration becomes unstable and demonstration of these mechanisms in simple models of a few degrees-of-freedom. These simple models often offer insight into friction-induced unstable vibration. Some of them were reported in [12, 15, 16, 23-30]. Popp and Stelter [12] studied the excitation mechanism of a violin string and revealed chaotic behaviour of two discrete and two continuous models due to dry friction. In [26], the instability of a simple sliding oscillator with friction having a Stribeck characteristic was studied analytically, and the results matched well with experimental results. Luo and Thapa [27] analysed periodic motion and local instability of a simplified brake system analytically, which provided a good understanding of nonlinear and non-smooth vibration of brake systems. Andreaus and Casini [29] studied the responses of a single-degree-of-freedom model with dry friction. The influences of the constant speed of the moving base, the driving force and the friction model on the dynamic behaviour of the system were investigated. In [30], stick-slip and impact motion of a single-degree-of-freedom oscillator excited by a frictional moving base and restricted by a unilateral rigid or deformable obstacle was studied. Hoffmann et al. [15] examined in detail mode-coupling instability of a two-degree-of-freedom model through its complex eigenvalues and time-domain response. The role of viscous damping on the instability of mode-coupling oscillation was clarified in [24]. Von Wagner et al. [31] reviewed a number of small models and developed a new two-degree-of-freedom system including a rigid

rotating disc in point contact with two point-pads. The stability of the wobbling disc motion was studied for various values of key parameters (normal pre-load, rotating velocity and friction coefficient), which gives a clear insight into the causes of the instability of the friction-induced disc vibration. A recent study [32] suggested that the number of degrees-of-freedom should not be too small and the right modes must be included when a large model was reduced.

As most systems contain nonlinearity in reality, the research into nonlinear friction-induced vibration has been carried out through experimental, analytical [33] and numerical approaches [34-36]. One significant source of nonlinearity in friction-induced vibration is the contact. Usually its stiffness is represented by a polynomial type of nonlinear stiffness which allows some nonlinear techniques [35] to be used. Sinou and Jézéquel [16] studied the role of damping in mode coupling instability and the amplitude of limit cycle of a simple nonlinear two-degree-of-freedom model which had a cubic nonlinear contact stiffness in order to avoid bad design. Moreover in [36], both a linear and a cubic contact laws were used in a simplified disc model, which fitted the experimental results of compression force against deformation of the pad material under varying normal pressure.

The possibility of loss of contact was mentioned in [36, 37] but the effect of separation was not studied. One limitation of most previous studies of friction-induced vibration of small models is that contact between the two bodies in sliding contact is assumed to be maintained during vibration. As the unstable friction-induced vibration caused by the friction force at the contact interface grows, it is important to consider separation during the vibration, when friction temporarily disappears.

One notable area of work is friction impact oscillator exemplified by Leine et al. [38]. Dynamic contact was treated as linear complementary problem and a generic formulation was presented. Its main advantage was the capability of dealing with unilateral contact and separation in multibody dynamics. On the other hand, their formulation was in mathematical form that did not lead to an asymmetric stiffness matrix that was the cornerstone of the mathematical framework for brake

squeal. Their Simplified Friction Impact Oscillator (in section 5.1) ended as a one-degree-of-freedom system with mass, damping and stiffness depending on a geometric character of an angle and the friction coefficient. As a result, the system can become unstable above certain critical values of the friction coefficient.

In the present paper, the effects of separation and subsequent reattachment on the vibration amplitude of a nonlinear two-degree-of-freedom model are studied; moreover, the important roles of pre-load and nonlinearity in the stabilisation and vibration magnitude of the system are analysed. Very interesting results are found, even though the simplest type of friction law (Coulomb friction) is adopted. This deviates from another line of research in which very sophisticated friction models (such as in Saha et al. [39]) are involved. One shortcoming of [39] is that the normal degree-of-freedom was absent. Berger in his review paper [4] summarised experimental results in a number of papers that stressed the importance of having the normal degree-of-freedom.

In this paper, firstly a nonlinear two-degree-of-freedom model with a pre-compression force is introduced in Sections 2 and 3. In Section 4, eigenvalues of the Jacobian matrix of the linearised system are calculated and the effects of nonlinear stiffness as well as the pre-load (pre-compression force) on the stability of the model are analysed. In Section 5, separation and reattachment during vibration are investigated numerically. In particular the changes of vibration amplitudes at various loading and nonlinear stiffness values are compared between two cases when separation is considered and ignored. Finally, conclusions are drawn in Section 6.

2. The mechanical model

To reveal the effects of separation on and contributions of various system parameters to instability, a nonlinear two-degree-of-freedom model illustrated in Fig. 1 is developed from a classic linear coupled two-degree-of-freedom model [15]. The current model contains a point mass m which is compressed by a vertical compression force F to bring a rigid massless slider against a rigid belt

moving at a constant speed. The contact between the slider and the belt is unilateral and a linear spring k_2 and a nonlinear spring k_{nl} together represent contact stiffness. From a realistic point of view, vertical separation may happen between the contacting surfaces. The mass is constrained by a spring k_1 and a damper c_1 in the horizontal direction and by a grounded damper c_2 in the vertical direction. Moreover, a grounded spring k_3 is linked to the mass at a 45° angle relative to the horizontal direction, which couples vibration in both directions. Since the focus of this paper is on the influences of the nonlinear stiffness and separation on the instability, and friction characteristics are not of interest, a constant coefficient of friction μ at contact point is assumed. The coordinate system defined in this paper comprises of a horizontal axis denoted by *x* and a vertical axis denoted by *y*, and the zero point of the coordinate system defined in the paper is the position when the pre-compression force *F* (also called pre-load, and it is positive when acting in the downward direction) has not yet been applied and the horizontal spring has not deformed yet. And the static position of the mass after the pre-compression force *F* is applied is referred to as the original static state. Then the belt starts to move at a constant speed.

During vibration, if the mass and belt are in contact, then contact force *P* acting on the slider (positive when *P* is a compressive force) is expressed as:

$$P = -k_2 y - k_{\mathrm{nl}} y^3 \tag{1}$$

Since the friction force F_r in Fig.1 is assumed to be proportional to the contact force *P*, expressed as $F_r = \mu P$, the equations of motion of this system can be expressed as:

$$\begin{bmatrix} m & 0 \\ 0 & m \end{bmatrix} \begin{bmatrix} \ddot{x} \\ \ddot{y} \end{bmatrix} + \begin{bmatrix} c_1 & 0 \\ 0 & c_2 \end{bmatrix} \begin{bmatrix} \dot{x} \\ \dot{y} \end{bmatrix} + \begin{bmatrix} k_1 + \frac{k_3}{2} & -\frac{k_3}{2} + \mu k_2 \\ -\frac{k_3}{2} & k_2 + \frac{k_3}{2} \end{bmatrix} \begin{bmatrix} x \\ y \end{bmatrix} + \begin{bmatrix} 0 & \mu k_{\mathrm{nl}} \\ 0 & k_{\mathrm{nl}} \end{bmatrix} \begin{bmatrix} x^3 \\ y^3 \end{bmatrix} = \begin{bmatrix} 0 \\ -F \end{bmatrix} \tag{2}$$

As the main purpose of this paper is to study the effects of the pre-load and nonlinear stiffness, other basic parameters of this system are taken as constants: m = 5, k_1 =100, k_2 =50, k_3=60; and c_1 =c_2=0.32, which means mass-proportional damping.

It should be stressed that the above equations of motion Eq. (2) are valid only if the following condition is satisfied:

$$P\,(t)\ >\ 0 \tag{3}$$

If loss of contact happens during vibration, contact stiffness k_2 and k_{nl} no longer make contributions to the system during separation, and then the system is governed by another set of equations of motion, to be discussed in Section 3.

3. Separation and reattachment

During vibration, it is necessary to check whether the slider separates from the moving belt or remains in contact with it. As the contact surface of the belt is assumed to be rigid in this model, the condition for staying in separation only depends on the vertical motion of the vibrating mass m, which is given by Eq. (4):

$$y\,(t)\ >\ 0 \tag{4}$$

Then the equations of motion for the mass during separation are given by Eq. (5):

$$\begin{bmatrix} m & 0 \\ 0 & m \end{bmatrix}\begin{bmatrix} \ddot{x} \\ \ddot{y} \end{bmatrix} + \begin{bmatrix} c_1 & 0 \\ 0 & c_2 \end{bmatrix}\begin{bmatrix} \dot{x} \\ \dot{y} \end{bmatrix} + \begin{bmatrix} k_1 + \frac{k_3}{2} & -\frac{k_3}{2} \\ -\frac{k_3}{2} & \frac{k_3}{2} \end{bmatrix}\begin{bmatrix} x \\ y \end{bmatrix} = \begin{bmatrix} 0 \\ -F \end{bmatrix} \tag{5}$$

The initial conditions for these equations are calculated from Eq. (2) at the last moment in contact.

After separation, the condition for maintaining separation, Eq. (4), is checked in order to find out the exact moment for reattachment. During separation, the contact force is zero, and sliding friction

force vanishes, so the states of the mass are calculated by a new set of equations of motion of the mass, Eq. (5). Then the vertical displacement $y(t)$ of the mass is monitored at the end of each time step. The condition for reattachment is when y (t) becomes zero, which means that the mass is vibrating downward back to the original static position. At this moment, the slider is just touching the moving belt without any contact force. So If $y(t) > 0$, separation is maintained. If $y(t)$ becomes negative at the end of a time step, then the bisection method is used to find the critical point, at which $y(t)$ is very near zero satisfying the defined tolerance in the Matlab codes, where the dynamics switches from separation phase to reattachment phase. After reattachment, the equations of motion of this system switch to Eq. (2) until the condition of separation is satisfied again and the initial conditions are calculated from Eq. (5) at the last step before reattachment. This scenario of switching between contact and separation can be repeated. A system like this is non-smooth.

For the sake of simplicity, the effects of impact at reattachment are neglected as in a different vibration problem involving contact but without friction [40].

4. Stability analysis

In this section, firstly the equilibrium points of the system are determined by solving the nonlinear equations in the static condition. Then the local linear approximation about the equilibrium points is used to obtain the Jacobian matrix of the linearised system which also preserves the distinct stability behaviour of the original nonlinear system [41, 42]. Finally the eigenvalues of the Jacobian matrix of this system are calculated in order to study the local instability of the system at the equilibrium points for various values of parameters.

4.1 Equilibrium points

The equilibrium points (x_e, y_e) are the solutions of the algebraic Eq. (6). As Eq. (6) here is a set of nonhomogeneous equations due to the pre-load term, equilibrium points are usually determined numerically.

$$\begin{bmatrix} k_1+\frac{k_3}{2} & -\frac{k_3}{2}+\mu k_2 \\ -\frac{k_3}{2} & k_2+\frac{k_3}{2} \end{bmatrix} \begin{bmatrix} x_e \\ y_e \end{bmatrix} + \begin{bmatrix} 0 & \mu k_{nl} \\ 0 & k_{nl} \end{bmatrix} \begin{bmatrix} x_e^3 \\ y_e^3 \end{bmatrix} = \begin{bmatrix} 0 \\ -F \end{bmatrix} \tag{6}$$

Though there are three roots of Eq. (6), only one root has the physical meaning because the other two are a pair of complex conjugates. The numerical results show that the static position represented by x_e and y_e are non-zero whose values are affected by the normal pre-compression force and the nonlinear stiffness. Fig. 2 (a)-(b) presents the evolutions of the equilibrium points with respect to the normal pre-compression force F and nonlinear stiffness k_{nl}. Fig. 2 (a) shows that the vertical positions of the equilibrium points decrease with the increasing pre-compression force, and a larger nonlinear stiffness value offers more resistance to the vertical displacement shown in Fig. 2 (b). On the other hand, Fig. 2 (b) shows that if there is no pre-compression force, the nonlinear stiffness would not affect the equilibrium positon. This means that the pre-compression force not only contributes to the system dynamics independently but also makes the nonlinear stiffness affect the equilibrium points of the nonlinear system. Thus the normal pre-compression force is an important factor for the equilibrium points of the original nonlinear system.

4.2 Eigenvalue analysis of the linearised system

In order to use the linear approximation method, Eq. (2) is converted into a set of first-order differential equations. By using the transformation relationships $z_1=x$, $z_2=\dot{x}$, $z_3=y$, $z_4=\dot{y}$, Eq. (2) is transformed into Eq. (7):

$$\begin{bmatrix}\dot{z}_1\\ \dot{z}_2\\ \dot{z}_3\\ \dot{z}_4\end{bmatrix}=\begin{bmatrix}0 & 1 & 0 & 0\\ -\frac{k_1+\frac{k_3}{2}}{m} & -\frac{c_1}{m} & -\frac{-\frac{k_3}{2}+\mu k_2}{m} & 0\\ 0 & 0 & 0 & 1\\ \frac{k_3}{2m} & 0 & -\frac{k_2+\frac{k_3}{2}}{m} & -\frac{c_2}{m}\end{bmatrix}\begin{bmatrix}z_1\\ z_2\\ z_3\\ z_4\end{bmatrix}+\begin{bmatrix}0 & 0 & 0 & 0\\ 0 & 0 & -\frac{\mu k_{\mathrm{nl}}}{m} & 0\\ 0 & 0 & 0 & 0\\ 0 & 0 & -\frac{k_{\mathrm{nl}}}{m} & 0\end{bmatrix}\begin{bmatrix}z_1^3\\ z_2^3\\ z_3^3\\ z_4^3\end{bmatrix}+\begin{bmatrix}0\\ 0\\ 0\\ -\frac{F}{m}\end{bmatrix} \tag{7}$$

By expanding the nonlinear equations in a first order truncated Taylor series at the equilibrium point [41, 42], the Jacobian matrix is given by Eq. (8):

$$J=\begin{bmatrix}0 & 1 & 0 & 0\\ -\frac{k_1+\frac{k_3}{2}}{m} & -\frac{c_1}{m} & -\frac{-\frac{k_3}{2}+\mu k_2}{m}-3\frac{\mu k_{\mathrm{nl}}}{m}y_{\mathrm{e}}^2 & 0\\ 0 & 0 & 0 & 1\\ \frac{k_3}{2m} & 0 & -\frac{k_2+\frac{k_3}{2}}{m}-3\frac{k_{\mathrm{nl}}}{m}y_{\mathrm{e}}^2 & -\frac{c_2}{m}\end{bmatrix} \tag{8}$$

The stability is manifested by the real parts of the eigenvalues λ of the Jacobian matrix. These eigenvalues reflect the features of the local stability at the equilibrium point (x_{e}, y_{e}). If all the real parts of the eigenvalues are negative, the system is stable; otherwise, as long as the real part of any eigenvalues is positive, the equilibrium point is unstable.

It can be noted that, because y_{e} takes non-zero values, the nonlinear stiffness terms appear in Eq. (8), unlike in other similar systems, for example, in [16]. For those systems having zero value as an equilibrium point, the nonlinear terms do not make contributions to the Jacobian matrix of the linearised system.

By setting the friction coefficient μ as a control parameter, the changes of the bifurcation points of this system are studied for various values of the normal pre-compression force and the nonlinear stiffness. In this paper, the friction coefficient satisfying the following condition Eq. (9) for bifurcation is called the critical friction coefficient μ_{c}.

$$\mathrm{Max}(\mathrm{Re}(\lambda)|_{\mu=\mu_{\mathrm{c}}})=0 \tag{9}$$

Bifurcation behaviour is illustrated in Figs. 3 and 4. Figs. 3 and 4 show the results of eigenvalue analysis with proportional damping (c_1=c_2=0.32), in which frequency and growth rate are the imaginary part and real part of the eigenvalue respectively. Friction coefficient μ is the control parameter. There are two distinct imaginary parts and modes, and the real parts are negative when μ <μ_c. With the increase of μ, the two imaginary parts and modes merge together at μ_c, and at the same time one of the real parts becomes zero. After the bifurcation point, one of the real parts becomes positive, as shown in Figs. 3 and 4. Thus these results indicate that the system is stable when μ< μ_c, and is unstable when μ> μ_c. The scenario depicted in Figs. 3 and 4 illustrates the well-known mode-coupling mechanism of unstable friction-induced vibration.

As shown in Figs. 3 and 4, μ_c changes with the nonlinear stiffness. Moreover, the evolution of μ_c with the nonlinear stiffness is found to be non-uniform for different values of the pre-compression force if one compares the results in Fig. 3 and Fig. 4. In Fig. 3 (F=20 N), the critical friction coefficient μ_c becomes smaller with the increasing nonlinear stiffness, and μ_c (coloured non-solid lines) are smaller than those of the linear system (black solid line). However, when the normal force is greater (F=100 N), as shown in Fig. 4, for the nonlinear system μ_c increases with the increasing nonlinear stiffness (k_{nl} =50, 100, 500 N/m^3), while the relation between μ_c of the nonlinear system (coloured non-solid lines) and μ_c of the linear system (black solid line) is complicated. For the case of k_{nl} =500 N/m^3, μ_c of the nonlinear system is greater than μ_c of the linear system, but μ_c of the nonlinear system in other cases (k_{nl} =50, 100 N/m^3) are smaller than μ_c of the linear system.

In the case of non-proportional damping (c_1=0.8, c_2=0.32), there are two distinct imaginary parts and modes when μ<μ_c, and the real parts are negative, which shows the same features as the proportional damping case. With the increase of μ, one of the real parts becomes zero at μ_c, while the two imaginary parts and modes get closer but do not coalesce. Similarly to the proportional damping case, one of the real parts becomes positive after the bifurcation point, as shown in Fig. 5.

To further examine the evolution of the critical friction coefficient in relation to the pre-compression force F, eigenvalue analysis for various values of F is carried out. The linear stiffness values are: k_1 =100 N/m, k_2 =50 N/m and k_3=60 N/m, which are identical to those used in getting the previous results. The results below are calculated by using proportional damping (c_1=c_2=0.32) because the results of non-proportional damping case give the same trend. In Fig. 6, the vertical axis is the critical friction coefficient μ_c for bifurcation and the horizontal axis is the varying values of the pre-compression force F. The results shown by the solid black line indicate that the normal pre-compression force does not influence the stability of the linear system, as the values of the critical friction coefficient stay the same. However, when the system is nonlinear (k_{nl} =50, 200, 500 N/m^3) shown by the colour non-solid lines, both nonlinear stiffness and pre-compression force influence the stability of this system. With the increasing normal pre-compression force, the nonlinear system （colour non-solid lines）firstly is more unstable compared with its corresponding linear system since the critical friction coefficient of the nonlinear system is smaller; then at a certain value of the normal pre-compression force (which depends on the value of the nonlinear stiffness), μ_c starts to increase with the increasing normal pre-compression force. Moreover, in the case of a large nonlinear stiffness value of k_{nl} =500 N/m^3 (the yellow dotted line), within the observation range of the normal pre-compression force, its μ_c finally becomes larger than the critical friction coefficient of the linear system (black solid line), which means that the nonlinear system under theses parameter values can become more stable than its corresponding linear system.

For a better understanding of the effects of nonlinear stiffness on the stability of this system, the evolution of μ_c against the nonlinear stiffness is studied. The numerical results are illustrated in Fig. 7. It is observed that when there is no normal pre-compression force in the system (shown by the solid black line), the nonlinear stiffness makes no contributions to the stability of the system. In the other cases with pre-load (F =5, 50,100 N) shown by coloured non-solid lines, by setting their

friction coefficient μ as the same as the linear system (shown by the solid black line), the nonlinear system firstly becomes more unstable as its μ_c decreases with the nonlinear stiffness; In the case of a large pre-load (F =100 N) shown by the yellow dotted line, the nonlinear system becomes more stable than the linear system when the nonlinearity is strong. However, when the pre-load is small (F=5 N) shown by the blue dashed line in Fig. 7, the nonlinear system is less stable than its linear system. For example, when μ equals to 1.2, the linear system is unstable as its μ_c is smaller than 1.2. On the other hand, the nonlinear system can be stabilised when the pre-load is increased to 100 N while the nonlinear stiffness k_{nl} equals 300 N/m^3 is introduced.

On the other hand, if the horizontal linear stiffness takes sufficiently smaller values than the values of vertical linear stiffness, for example, k_1 =50 N/m and k_2 =100 N/m, the changes of the critical friction coefficient with the values of the normal pre-compression force and nonlinear stiffness, in Figs. 8 and 9, show different behaviour from the results when k_1=100 N/ m and k_2=50 N/ m. Basically, when k_1 =50 N/ m and k_2 =100 N/ m, the nonlinear system is always more stable than its corresponding linear part. Moreover, with the increase of F and the k_{nl}, the stability of the nonlinear system is enhanced in a monotonic trend.

Consequently, the stability of the nonlinear coupled system with sliding friction is much more complex than the corresponding linear system. Parametric studies show that the nonlinear stiffness as well as the pre-compression force plays important roles in the stabilisation of the system. When nonlinear stiffness and pre-compression force are introduced into the system, they firstly make the system unstable, which is not an intuitive conclusion; however, in the cases of strong nonlinearity or large normal compression force, certain combinations of the nonlinear stiffness and the normal pre-compression force stabilise the original unstable system. These phenomena can be exploited for controlling friction-induced vibration. On the other hand, the values of the linear stiffness of a

nonlinear system are also important as they can influence how the nonlinear stiffness and the normal pre-compression force affect the stability of this nonlinear system.

5. Dynamic transient analysis

In order to find out the influence of separation on the dynamic behaviour of the nonlinear system, time domain responses are calculated numerically for various values of the key parameters. A nonlinear system can become stable or unstable depending on the values of the system parameters, which has been discussed in Section 4. It is found that separation does not occur for a stable system in most situations; and even if separation happens under some conditions, the vibration of the system still gradually decreases and eventually gets back to the equilibrium point, which is not of interest in this paper. Also due to the page limitation, these results will not be given in this paper. Thus this section mainly focuses on the vibration of the unstable system considering separation. Firstly through a numerical example, the occurrence of separation during vibration is illustrated; then the influences of nonlinear stiffness and normal pre-compression force on the friction-induced vibration considering separation are investigated; finally the role of separation on the vibration amplitude is analysed through the comparisons between the results of two cases: (1) separation is considered; (2) separation is ignored.

5.1 Separation during vibration

In this paper, the fourth-order Runge-Kutta method appropriate for the second-order differential equations [43] is used to calculate the transient responses of the nonlinear system numerically. As the state of the system switches between separation and in-contact phases, the dynamic behaviour of the system needs to be obtained by solving two different sets of governing equations, which brings about some difficulties, such as determining the motion state and searching for the transition point for the two distinct states, in the numerical computation. The process of the numerical computation is as follows: The equations of motion are given by Eq. (2). The contact force is checked at the end

of every single time step during numerical computation. The tracking of separation and reattachment follows the conditions given in Section 3. If during the in-contact phase the contact force $P(t)$ drops below zero at the end of a time step, the bisection method is used to find the critical contact force satisfying the error tolerance defined in the algorithm and the associated motion states (displacement, velocity and acceleration). Then separation is considered to take place and the equations of motion are now given by Eq. (5). Separation ceases when the mass moves downwards to y=0. If during the separation phase y drops below zero at the end of a time step, the bisection method is used to find the critical point for reattachment. Then the slider re-establishes contact with the moving belt again and Eq. (2) is now back in charge until the next separation happens. Impact that may occur at the reattachment [44-45] is ignored in this paper, as the time duration of separation is short, so impact may influence the vibration only slightly; in this paper the main interest is in the effects of significant parameters on dynamics of friction-induced vibration problem; in future work, more factors including impact will be considered.

The parameter values in this numerical example are: k_1 =100; k_2 =50; k_3=60; F=80; k_{nl}=100; μ=0.7. The critical friction coefficient μ_c for bifurcation with theses parameters is 0.28. The numerical results are given in Figs. 10 – 12.

Fig.10 shows that the fluctuation ranges of the contact forces during vibration of the two cases: separation is ignored and is considered. It can be noticed that the contact force (shown by the blue solid line) gradually grows and becomes negative when separation is ignored. This means that the results of the ignoring- separation case are not realistic as the contact force should always be non-negative. For the case when separation is considered (shown by the green dashed line), multi-separation events can be observed as the values of contact force repeat the following process during the vibration: drop to zero (transition from in-contact state to separation state), remain zero (during separation), become positive (in-contact) and drop to zero again. As both the contact

stiffness and friction force are absent during separation, the motion of the slider and the mass as a whole is governed by Eq. (5). Figs. 11 and 12 show that separation makes both the horizontal and vertical motion different from their counterparts when separation is ignored. Meanwhile the vibration and the fluctuating contact force are asymmetric about the original static state when loss of contact is considered. In conclusion, even in the presence of the normal pre-compression force as a pre-load, separation still can take place during vibration, and reattachment naturally occurs with separation.

5.2 *Effects of separation on the amplitudes*

To assess the influences of separation on the maximum vibration amplitude of the nonlinear friction-induced vibration, comparisons between cases of separation being considered (Case 1) and ignored (Case 2) are made through a parametric study for various values of nonlinear stiffness and normal pre-compression force.

Firstly, the changes in the maximum amplitudes of the vertical vibration of the mass are obtained by varying the values of the normal pre-compression force while keeping the nonlinear stuffiness as a constant. The results are shown in Figs. 13 (k_{nl} =20 N/m^3 and μ=0.5) and 14 (k_{nl} =100 N/m^3 and μ=0.7). These values are chosen based on the results of the eigenvalue analysis in Section 4, under which typical unstable motion of the mass can be obtained. The blue solid line represents the case when loss of contact is ignored; the green dashed line is for the case when separation and reattachment are considered.

As shown in Fig. 13, a significant difference in the roles of the normal pre-compression force on the vibration amplitude can be observed between Case 1 and Case 2. When separation is ignored (blue solid line) in Fig.13, the normal pre-load barely affects the maximum amplitude of the nonlinear vibration. In contrast, for the more realistic case when separation is considered (the green dashed line) in Fig. 13, the maximum vibration amplitude of the mass becomes larger with the increasing

normal pre-compression force, which is not an intuitive expectation that increasing the normal pre-compression force leads to greater vibration. Moreover, at the initial increase of the normal pre-load, the maximum amplitudes are smaller than those in Case 2 (separation ignored). However, at a larger pre-compression force, the situation is reversed.

For the nonlinear system having a stronger nonlinear contact spring shown in Fig. 14, a similar trend of the maximum amplitudes to that of Fig. 13 is found, and the maximum amplitudes in Case 1 exceed those of Case 2 at a much lower value of the normal compression force. This means that ignoring separation during the vibration underestimates the vibration, which is unsafe for the system.

Then Figs. 15 and 16 show the changes of maximum vibration amplitude with respect to the nonlinear contact stiffness in two pre-load cases. Normal compression forces in Figs. 15 and 16 are 40 N and 60 N, and μ is 0.7 and 1 respectively. The results clearly show that, if separation is not considered (blue solid line), the nonlinear contact stiffness appears stabilising. As separation does happen during the vibration, in fact the results with separation considered indicate that larger contact stiffness induces greater vibration, as shown in Figs. 15 and 16. Moreover, in Fig.15, the maximum amplitudes in Case 1 (separation considered) initially are smaller than in Case 2 (separation ignored) at the same nonlinear stiffness value, but they tend to become larger than in Case 2 when the nonlinear stiffness is increased. In addition, the maximum amplitudes depend on the normal compression force, as shown in Fig. 16 (F=60 N), where even at a small value of nonlinear contact stiffness, the maximum amplitudes in Case 1 are greater.

The above apparently puzzling dynamic behaviour can be explained as follows. If separation is ignored, after the contact force becomes negative, the contact spring gets stretched and it still offers the resistance force hindering the mass from moving upward further, meanwhile the friction force still makes a contribution to the horizontal vibration. However, when separation is allowed, the

vertical contact stiffness is lost during separation which does not offer the same amount of resistance force to the vertical vibration; at the same time, the horizontal friction force disappears which will not make any contribution to the horizontal vibration. Also because the horizontal and vertical vibration is coupled, the vibration of this system when separation is considered is actually more complex. These are very interesting findings and can be exploited in control of friction-induced vibration.

Consequently, when the loss of contact is considered, the effects of the nonlinear stiffness and normal pre-compression force on the evolution of vibration amplitude are not the same as when separation is ignored. Given the very important contributions of separation found in this paper, it should be taken into account in models of friction-induced vibration. Flexibility of the moving belt and impact at reattachment after separation are other important factors to be considered in future.

Conclusions

In this paper, a two-degree-of-freedom mass-slider on moving belt model for vibration induced by sliding friction is developed. A cubic nonlinear spring is introduced at the contact point between the slider and the belt. The equations of motion at two vibration states (when the slider and the belt are in contact and in separation) are derived and conditions for separation and reattachment after separation are given.

The effects of nonlinear contact stiffness as well as the normal pre-load on the local stability near the equilibrium point are studied by the eigenvalue analysis. The results of both proportional damping and non-proportional damping cases show that, the roles of nonlinear stiffness and the pre-load on the stability of the system are complicated. Initially, increasing the nonlinear stiffness or the pre-load tends to make the nonlinear system more unstable than the linear system; but at certain higher values, they start to stabilise the system; at some even higher values, the nonlinear system is more stable than its corresponding linear system with the same friction coefficient. These properties

can be taken advantage of in controlling friction-induced vibration. Additionally, the influence of the nonlinear stiffness and the pre-load in this nonlinear system can be different, depending on the values of the linear stiffness.

Through numerical studies, the process of contact loss and reattachment of the slider during vibration is demonstrated. It is found that separation can happen even under a large pre-load. Moreover, when separation is considered, not only the change of vibration amplitudes against some system parameter values is opposite to the trend when separation is ignored, but also the values of the amplitudes are larger in certain conditions. Therefore, ignoring separation, as always occurs in simple models for friction-induced vibration, is likely to under-predict vibration magnitude and thus is unsafe. Therefore a major conclusion is that separation at the contact interface should be taken into account in the nonlinear friction-induced vibration problem.

Acknowledgments

The first author is grateful for the University of Liverpool-China Scholarship Council scholarship.

References

[1] Akay, A., 2002, "Acoustics of friction," J. Acoust. Soc. Am., **111**(4), pp. 1525-1548.

[2] Ibrahim, R. A., 1994, "Friction-Induced Vibration, Chatter, Squeal, and Chaos—Part I: Mechanics of Contact and Friction," ASME Appl. Mech. Rev., **47**(7), pp. 209-226.

[3] Ibrahim, R. A., 1994, "Friction-Induced Vibration, Chatter, Squeal, and Chaos—Part II: Dynamics and Modeling," ASME Appl. Mech. Rev., **47**(7), pp. 227-253.

[4] Berger, E. J., 2002, "Friction modeling for dynamic system simulation," ASME Appl. Mech. Rev., **55**(6), pp. 535-577.

[5] Kinkaid, N. M., O'Reilly, O. M., and Papadopoulos, P., 2003, "Automotive disc brake squeal," J. Sound Vib., **267**(1), pp. 105-166.

[6] Ouyang, H., Nack, W., Yuan, Y., and Chen, F., 2005, "Numerical analysis of automotive disc brake squeal: a review," IJVNV, **1**(3-4), pp. 207-231.

[7] Elmaian, A., Gautier, F., Pezerat, C., and Duffal, J. M., 2014, "How can automotive friction-induced noises be related to physical mechanisms?," Appl. Acoust., **76**, pp. 391-401.

[8] Mills, H. R., 1938, "Brake squeak," Technical report 9000 B, Institution of Automobile Engineers.

[9] Spurr, R. T., 1961, "A theory of brake squeal," Proc. Automob. Div. Inst. Mech. Eng, pp. 33-52.

[10] Hoffmann, N., and Gaul, L., 2004, "A sufficient criterion for the onset of sprag-slip oscillations," Arch. Appl. Mech., **73**(9-10), pp. 650-660.

[11] Sinou, J. J., Thouverez, F., and Jezequel, L., 2003, "Analysis of friction and instability by the centre manifold theory for a non-linear sprag-slip model," J. Sound Vib., **265**(3), pp. 527-559.

[12] Popp, K., and Stelter, P., 1990, "Stick-Slip Vibrations and Chaos," Philos. Trans. Roy. Soc. A, **332**(1624), pp. 89-105.

[13] Luo, A. C. J., and Gegg, B. C., 2006, "On the mechanism of stick and nonstick, periodic motions in a periodically forced, linear oscillator with dry friction," ASME J. Vib. Acoust., **128**(1), pp. 97-105.

[14] North, N. R., 1976, "Disc brake squeal," Proc. Inst. Mech. Eng., **C38/76**, pp. 169–176.

[15] Hoffmann, N., Fischer, M., Allgaier, R., and Gaul, L., 2002, "A minimal model for studying properties of the mode-coupling type instability in friction induced oscillations," Mech. Res. Commun., **29**(4), pp. 197-205.

[16] Sinou, J.-J., and Jézéquel, L., 2007, "Mode coupling instability in friction-induced vibrations and its dependency on system parameters including damping," Eur. J. Mech. A/Solid., **26**(1), pp. 106-122.

[17] Duffour, P., and Woodhouse, J., 2004, "Instability of systems with a frictional point contact. Part 1: basic modelling," J. Sound Vib., **271**, pp. 365-390.

[18] Chan, S. N., Mottershead, J. E., and Cartmell, M. P., 1994, "Parametric resonances at subcritical speeds in discs with rotating frictional loads," Proc. Inst. Mech. Eng. Part C (J. Mech. Eng. Sci.), **208**(6), pp. 417-425.

[19] Ouyang, H., Mottershead, J. E., and Li, W., 2003, "A moving-load model for disc-brake stability analysis," ASME J. Vib. Acoust., **125**(1), pp. 53-58.

[20] Jarvis, R. P., and Mills, B., 1963, "Vibrations Induced by Dry Friction," Proc. Inst. Mech. Eng., **178**(1), pp. 847-857.

[21] Flint, J., and HultÉN, J., 2002, "Lining-deformation-induced modal coupling as squeal generator in a distributed parameter disc brake model," J. Sound Vib., **254**(1), pp. 1-21.

[22] Ouyang, H., and Mottershead, J. E., 2005, "Dynamic Instability of an Elastic Disk Under the Action of a Rotating Friction Couple," J. Appl. Mech., **71**(6), pp. 753-758.

[23] Kinkaid, N. M., O'Reilly, O. M., and Papadopoulos, P., 2005, "On the transient dynamics of a multi-degree-of-freedom friction oscillator: a new mechanism for disc brake noise," J. Sound Vib., **287**(4–5), pp. 901-917.

[24] Hoffmann, N., and Gaul, L., 2003, "Effects of damping on mode-coupling instability in friction induced oscillations," ZAMM Z. Angew. Math. Mech., **83**(8), pp. 524-534.

[25] Li, Y., and Feng, Z. C., 2004, "Bifurcation and chaos in friction-induced vibration," Commun. Nonlinear Sci. Numer. Simul., **9**(6), pp. 633-647.

[26] Hetzler, H., Schwarzer, D., and Seemann, W., 2007, "Analytical investigation of steady-state stability and Hopf-bifurcations occurring in sliding friction oscillators with application to low-frequency disc brake noise," Commun. Nonlinear Sci. Numer. Simul., **12**(1), pp. 83-99.

[27] Luo, A. C. J., and Thapa, S., 2009, "Periodic motions in a simplified brake system with a periodic excitation," Commun. Nonlinear Sci. Numer. Simul., **14**(5), pp. 2389-2414.

[28] Shin, K., Brennan, M. J., Oh, J. E., and Harris, C. J., 2002, "Analysis of disc brake noise using a two-degree-of-freedom model," J. Sound Vib., **254**(5), pp. 837-848.

[29] Andreaus, U., and Casini, P., 2001, "Dynamics of friction oscillators excited by a moving base and/or driving force," J. Sound Vib., **245**(4), pp. 685-699.

[30] Andreaus, U., and Casini, P., 2002, "Friction oscillator excited by moving base and colliding with a rigid or deformable obstacle," Int. J. Non-Linear Mech., **37**(1), pp. 117-133.

[31] von Wagner, U., Hochlenert, D., and Hagedorn, P., 2007, "Minimal models for disk brake squeal," J. Sound Vib., **302**(3), pp. 527-539.

[32] Butlin, T., and Woodhouse, J., 2009, "Friction-induced vibration: Should low-order models be believed?," J. Sound Vib., **328**(1-2), pp. 92-108.

[33] D'Souza, A. F., and Dweib, A. H., 1990, "Self-excited vibrations induced by dry friction, part 2: Stability and limit-cycle analysis," J. Sound Vib., **137**(2), pp. 177-190.

[34] Ouyang, H., Baeza, L., and Hu, S., 2009, "A receptance-based method for predicting latent roots and critical points in friction-induced vibration problems of asymmetric systems," J. Sound Vib., **321**(3–5), pp. 1058-1068.

[35] Sinou, J. J., Thouverez, F., and Jézéquel, L., 2004, "Methods to reduce non-linear mechanical systems for instability computation," Arch. Comput. Method Eng., **11**(3), pp. 257-344.

[36] Soobbarayen, K., Sinou, J. J., and Besset, S., 2014, "Numerical study of friction-induced instability and acoustic radiation – Effect of ramp loading on the squeal propensity for a simplified brake model," J. Sound Vib., **333**(21), pp. 5475-5493.

[37] Brunetti, J., Massi, F., D'Ambrogio, W., and Berthier, Y., 2015, "Dynamic and energy analysis of frictional contact instabilities on a lumped system," Meccanica, **50**(3), pp. 633-647.

[38] Leine, R. I., Brogliato, B., and Nijmeijer, H., 2002, "Periodic motion and bifurcations induced by the Painlevé paradox," Eur. J. Mech. A/Solid., **21**(5), pp. 869-896.

[39] Saha, A., Wiercigroch, M., Jankowski, K., Wahi, P., and Stefański, A., 2015, "Investigation of two different friction models from the perspective of friction-induced vibrations," Tribol. Int., **90**, pp. 185-197.

[40] Lee, U., 1996, "Revisiting the Moving Mass Problem: Onset of Separation Between the Mass and Beam," ASME J. Vib. Acoust., **118**(3), pp. 516-521.

[41] Medio, A., and Lines, M., 2001, *Nonlinear dynamics: a primer*, Cambridge University Press, Cambridge.

[42] Meirovitch, L., 1990, *Dynamics and control of structures*, Wiley, New York.

[43] Pollard, H., and Tenenbaum, M., 1964, *Ordinary differential equations*, Harper & Row, New York.

[44] Andreaus, U., and Nisticò, N., 1998, "An analytical-numerical method for contact-impact problems. Theory and implementation in a two-dimensional distinct element algorithm," Comput. Model. Simul. Engrg., **3**(2), pp. 98-110.

[45] Baeza, L., and Ouyang, H., 2008, "Dynamics of a truss structure and its moving-oscillator exciter with separation and impact-reattachment," Proc. Roy. Soc. A: Math. Phys. Eng. Sci., **464**(2098), pp. 2517-2533.

Figure Caption List

Fig. 1 A two-degree-of-freedom model with nonlinear stiffness

Fig. 2 Vertical displacements of equilibrium points versus normal pre-compression force F (a) and nonlinear stiffness k_{nl} (b)

Fig. 3 The real (right) and imaginary part (left) of the eigenvalues versus the friction coefficient μ for various nonlinear stiffness. The imaginary parts are the frequencies and real parts are growth rates (F =20 N)

Fig. 4 The real (right) and imaginary part (left) of the eigenvalues versus the friction coefficient μ for various nonlinear stiffness. The imaginary parts are the frequencies and real parts are growth rates (F =100 N)

Fig. 5 The real (right) and imaginary part (left) of the eigenvalues versus the friction coefficient μ for various nonlinear stiffness with non-proportional damping. The imaginary parts are the frequencies and real parts are growth rates (F =100 N)

Fig. 6 Evolution of the critical friction coefficient against the pre-compression force

Fig. 7 Evolution of the critical friction coefficient against the nonlinear stiffness

Fig. 8 Evolution of the critical friction coefficient against the pre-compression force

Fig. 9 Evolution of the critical friction coefficient against the nonlinear stiffness

Fig. 10 Time-domain results of the contact force during the time period [0-100s]

Fig. 11 Time response of the horizontal displacement during the time period [0-100s]

Fig. 12 Time response of the vertical displacement during the time period [0-100s]

Fig. 13 Maximum vertical amplitudes against normal pre-compression forces (k_{nl} =20 N/m^3)

Fig. 14 Maximum vertical amplitudes against normal pre-compression forces (k_{nl} =100 N/m^3)

Fig. 15 Maximum vertical amplitudes for various nonlinear stiffness values (F=40 N)

Fig. 16 Maximum vertical amplitudes for various nonlinear stiffness values (F=60 N)

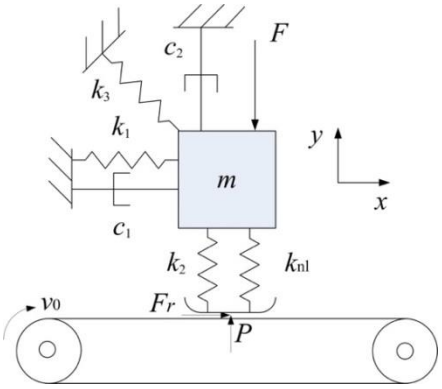

Fig. 1. A two-degree-of-freedom model with nonlinear stiffness

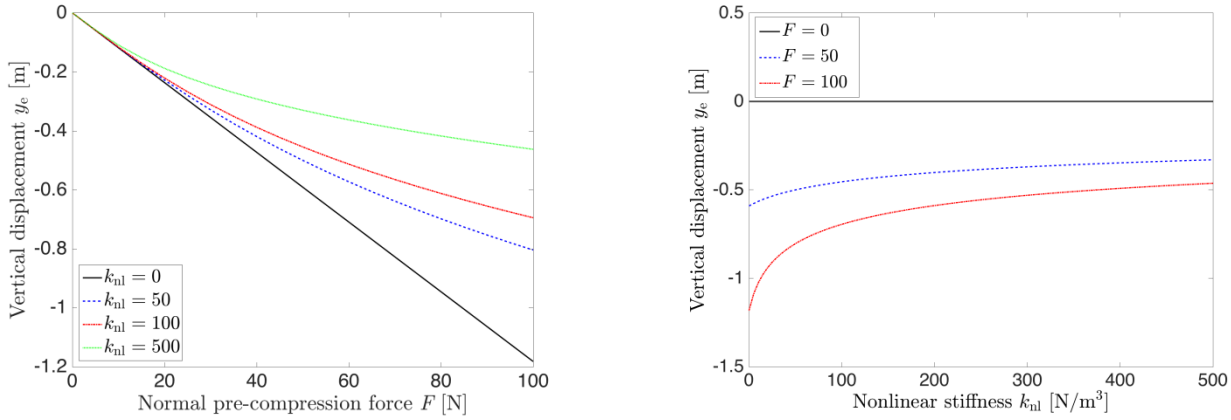

(a) (b)

Fig. 2. Vertical displacements of equilibrium points versus normal pre-compression force F (a) and nonlinear stiffness k_{nl} (b)

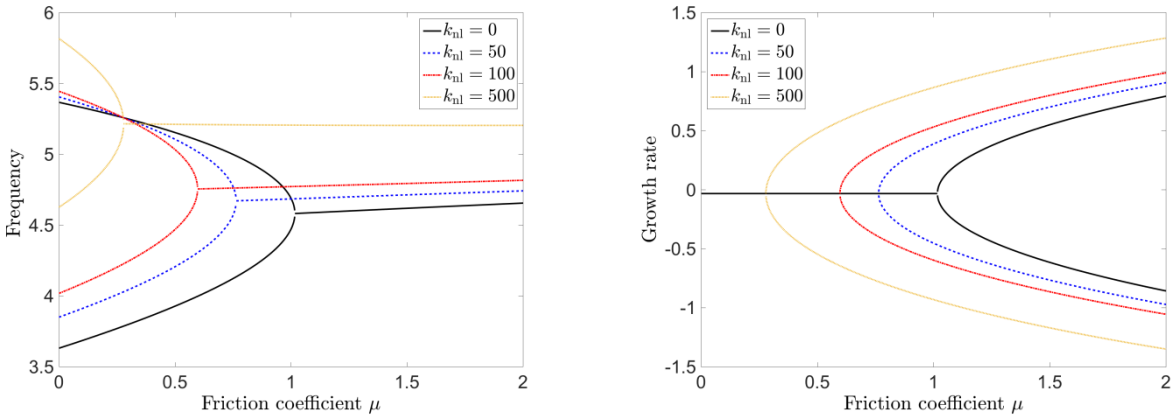

Fig. 3. The real (right) and imaginary part (left) of the eigenvalues versus the friction coefficient μ for various nonlinear stiffness.

The imaginary parts are the frequencies and real parts are growth rates (F =20 N)

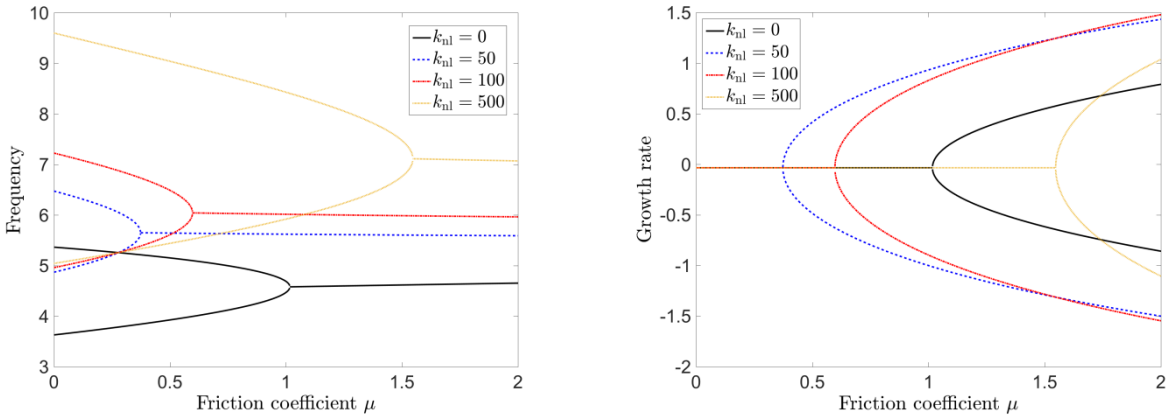

Fig. 4. The real (right) and imaginary part (left) of the eigenvalues versus the friction coefficient μ for various nonlinear stiffness.

The imaginary parts are the frequencies and real parts are growth rates (F =100 N)

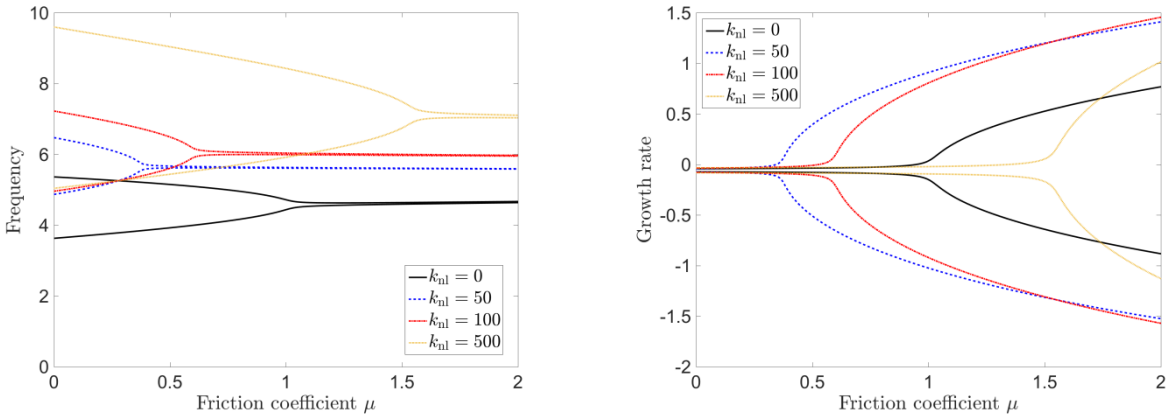

Fig. 5. The real (right) and imaginary part (left) of the eigenvalues versus the friction coefficient μ for various nonlinear stiffness with non-proportional damping. The imaginary parts are the frequencies and real parts are growth rates (F =100 N)

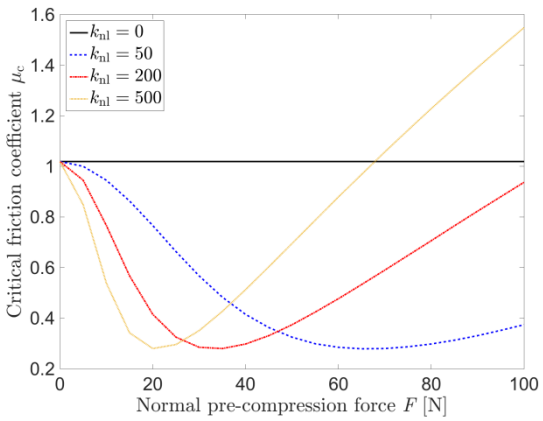

Fig. 6. Evolution of the critical friction coefficient against the pre-compression force

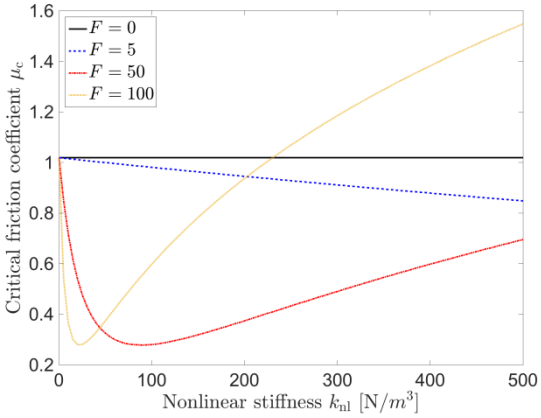

Fig. 7. Evolution of the critical friction coefficient against the nonlinear stiffness

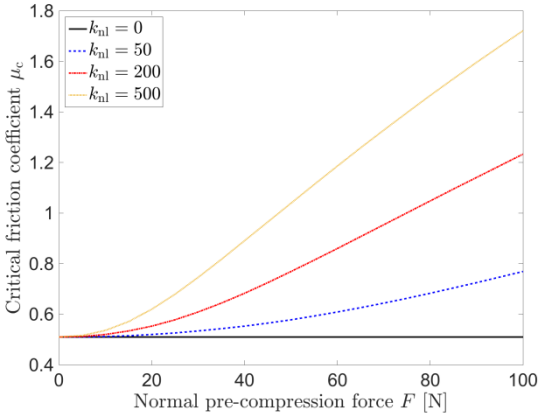

Fig. 8. Evolution of the critical friction coefficient against the pre-compression force

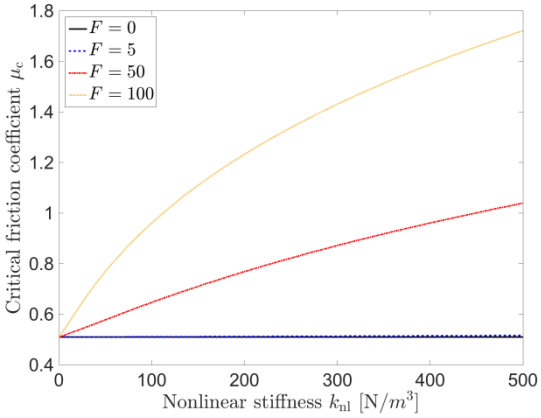

Fig. 9. Evolution of the critical friction coefficient against the nonlinear stiffness

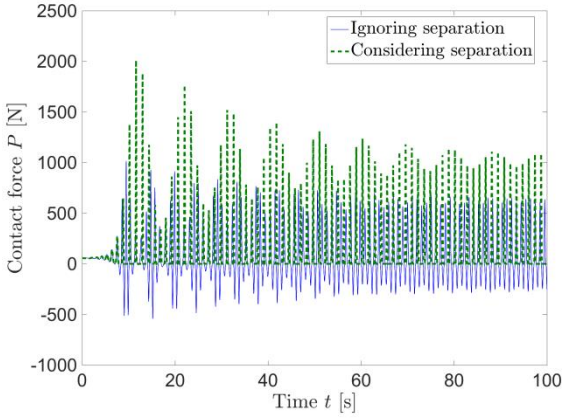

Fig. 10. Time-domain results of the contact force during the time period [0-100s]

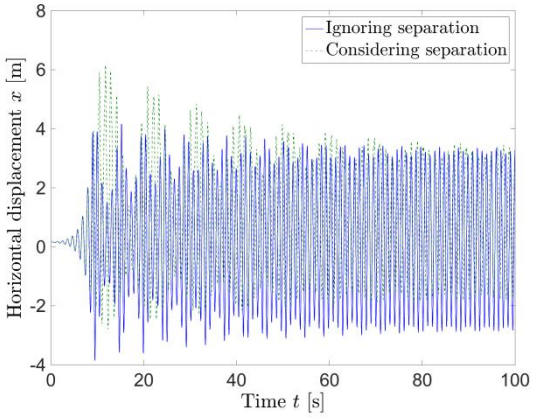

Fig. 11. Time response of the horizontal displacement during the time period [0-100s]

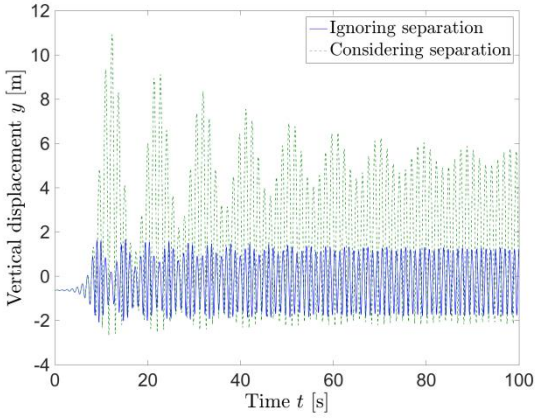

Fig. 12. Time response of the vertical displacement during the time period [0-100s]

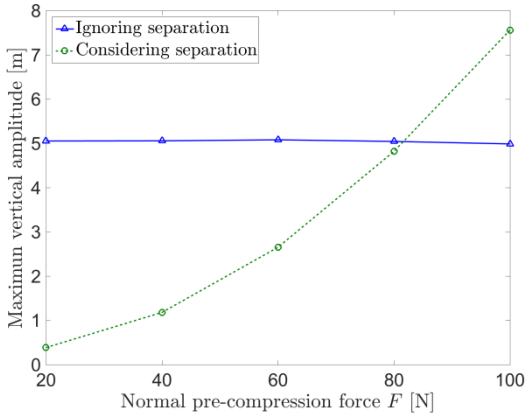

Fig. 13. Maximum vertical amplitudes against normal pre-compression forces (k_{nl} =20 N/m^3)

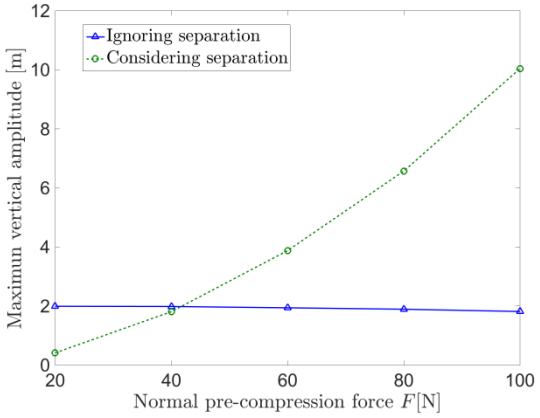

Fig. 14. Maximum vertical amplitudes against normal pre-compression forces (k_{nl} =100 N/m^3)

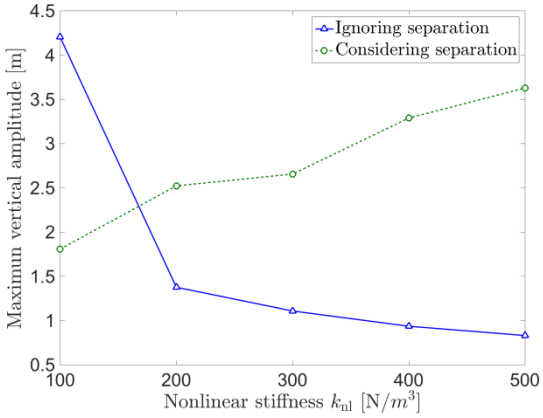

Fig. 15. Maximum vertical amplitudes for various nonlinear stiffness values (F=40 N)

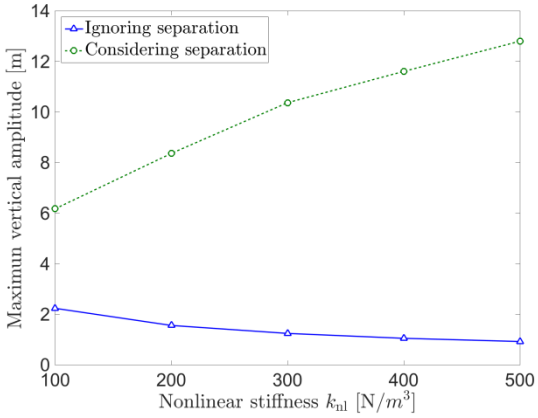

Fig. 16. Maximum vertical amplitudes for various nonlinear stiffness values (F=60 N)